Polymer 189 (2020) 122171

Contents lists available at ScienceDirect

Polymer

journal homepage: http://www.elsevier.com/locate/polymer

Tangled silver nanoparticles embedded polythiophene-functionalized multiwalled carbon nanotube nanocomposites with remarkable electrical and thermal properties

T.S. Swathy, M. Jinish Antony *

Research and PG Department of Chemistry, Centre for Sustainable Chemistry, St. Thomas College (Autonomous), Affiliated to University of Calicut, Thrissur, 680 001, Kerala, India

ARTICLE INFO

Keywords:
Ternary nanocomposites
Silver nanoparticles
Conducting polymers
Nanodispersions

ABSTRACT

Tangled silver nanoparticles embedded layered polythiophene-functionalized multiwalled carbon nanotube ternary nanocomposite (**PTCNT-COOH 300 Ag**) has been prepared by ascorbic acid reduction of silver nitrate solution in presence of aqueous dispersion of polythiophene-functionalized multiwalled carbon nanotube (**PTCNT-COOH**) binary nanocomposites. Binary polythiophene–functionalized multiwalled carbon nanotube nanocomposites have been prepared by *in-situ* chemical oxidative polymerization of thiophene monomer stabilized by sodium bis(2-ethylhexyl) sulfosuccinate (AOT) micelles in presence of functionalized multiwalled carbon nanotubes (**MWCNT-COOH**) using ferric chloride ($FeCl_3$) as an oxidizing agent in chloroform solvent. The structural formation and composition of binary and ternary nanocomposites have been confirmed by fourier transform infrared spectroscopy, fourier transform Raman spectroscopy, X-ray photoelectron spectroscopy (XPS) and wide angle X-ray diffraction studies. Scanning electron microscopy (SEM) studies have revealed the nanofibrous morphology in binary nanocomposites (**PTCNT-COOHs)**, whereas in ternary nanocomposite (**PTCNT-COOH 300 Ag**), silver nanoparticles were densely embedded as nanoparticles over nanofibrous structure. Transmission electron microscopic (TEM) images have provided the evidence regarding silver nanoparticles that existed in a tangled state over the nanofibrous structure. Stable dispersion of binary nanocomposites (**PTCNT-COOHs)** in water, ethanol and chloroform enabled us to record the UV–visible absorption spectra which have shown two peaks at 260 nm and 360 nm corresponding to π-π^* transition from aromatic rings and π-polaron absorption of polythiophene respectively. On the other hand, ternary nanocomposite have shown surface plasmon resonance as broad peak tailing to 550 nm. The electrical conductivity of nanocomposites **PTCNT-COOH 100 (**binary nanocomposite**), PTCNT-COOH 200 (**binary nanocomposite**), PTCNT-COOH 300** (binary nanocomposite), pristine **MWCNT,** functionalized **MWCNT-COOH, MWCNT-COOH Ag** (binary nanocomposite) and **PTCNT-COOH 300 Ag** (ternary nanocomposite) were 4.42×10^{-2}, 5.30×10^{-1}, 1.64, 8.66, 2.80, 12.40 and 80.76 S/cm respectively. The enhanced electrical conductivity of ternary nanocomposite was due to the effective charge transport through polythiophene layer which act as conductive bridge between multiwalled carbon nanotube and silver nanoparticles. Thermogravimetric analysis have revealed that high thermal stability of ternary silver nanocomposite of **PTCNT-COOH 300 Ag** up to 620 °C for 10% weight loss. Silver nanoparticles embedded ternary nanocomposite in basic medium shows least leaching effect, therefore it could be potentially useful in catalytical applications.

1. Introduction

Conducting polymer-carbon nanocomposite materials find several applications in technologically advanced research fields and hence there have been growing interest for the fabrication of binary or ternary conducting polymer-carbon nanocomposites [1–10]. The components of nanocomposites generally possess attractive features which could be imparted to the finished nanocomposites as an enhancement or modification [11–13]. Conducting polymers and multiwalled carbon nanotubes (MWCNTs) possess inherent properties such as optical, electrical,

* Corresponding author.
E-mail address: jinish06@yahoo.co.in (M. Jinish Antony).

https://doi.org/10.1016/j.polymer.2020.122171
Received 23 September 2019; Received in revised form 30 November 2019; Accepted 11 January 2020
Available online 12 January 2020
0032-3861/

mechanical and thermal properties at distinct levels. Diverse applications have been reported for such materials in electrical circuits and displays to power devices, super capacitors, micro-electro-mechanical systems (MEMS), solar cells, sensors, catalysis and so on [12,14–25]. Among different conducting polymer-carbon nanocomposites, polythiophene-multiwalled carbon nanotube nanocomposite system has interesting structural features, electrical and optical properties, thermal and bio compatibility etc [11,26–32]. Conducting polythiophene-multiwalled carbon nanotube nanocomposite materials are potentially suitable for polymer light emitting diodes, electrochemical sensors, energy storage devices, super capacitors, electromagnetic radiation shielding, photovoltaic devices and so on [33–36].

Polymer nanocomposites can be synthesized by in situ polymerization of monomer in the presence of CNT or functionalized CNT [37,38]. Functionalized multiwalled carbon nanotubes can act as effective synergistic host by the formation of core shell morphology with other materials via taking advantage of its large surface area [39,40]. Functionalized MWCNT with functional groups attached to the surface of MWCNT can undergo non-covalent interactions at the interface with other components to which it is attached. Functionalized MWCNT synthesized with properly controlled size, shape and functional groups can be utilized to produce stable dispersion, which can improve the processability of these materials tremendously in applications [41,42]. Further improvements in the performance of functional nanocomposites could be imparted by the addition of metal fillers into binary nanocomposites. Incorporation of metal nanoparticles as filler is an emerging frontier approach to enhance the performance of conducting polymer-carbon nanotube nanocomposites [43]. Although studies on polythiophene-carbon nanotube composite materials have been carried out by various researchers, incorporation of stable silver nanoparticles into polythiophene-functionalized multiwalled carbon nanotube was rarely reported. Patole et al. reported preparation of PEDOT/PSS-ethylenediamine functionalized multiwalled carbon nanotube-silver nanoparticle nanocomposite by reduction of $AgNO_3$ using $NaBH_4$ in dichloromethane for improving electrical conductivity and thermal properties of polycarbonate matrix [44]. Adopting green approaches can render a more facile pathway to prepare silver nanoparticles embedded polythiophene-functionalized multiwalled carbon nanotube with several advantageous over cost, efficiency and many other merits such as good dispersibility, high electrical conductivity and thermal stability. The performance of the nanocomposite materials in many applications heavily depends on the properties and processability.

In the present studies, we have put forward a facile and green synthetic approach for the development of silver nanoparticles embedded polythiophene-functionalized multiwalled carbon nanotube nanocomposites by the reduction of silver nitrate with ascorbic acid (Vitamin-C) in aqueous medium. Here, we have introduced chemically synthesized binary nanocomposite (**PTCNT-COOH 300**) as a nanofibrous template in which silver nanoparticles were allowed to embed as ternary nanocomposite. Here, the polythiophene-functionalized multiwalled carbon nanotube nanocomposite could act as stable framework to protect and accommodate highly labile silver atoms as solid nanoparticles, otherwise they agglomerate in the absence of strong capping agent. Interestingly, the tangled silver nanoparticles embedded polythiophene-functionalized MWCNT nanocomposite possess good dispersibility in water, high electrical conductivity, good solid state ordering and thermal stability.

2. Experimental

Materials and reagents: Thiophene, sodium bis (2-ethylhexyl) sulfosuccinate (AOT), ferric chloride, silver nitrate and multiwalled carbon nanotubes (MWCNT) were purchased from Sigma Aldrich. Nitric acid, ascorbic acid, sodium hydroxide, chloroform, deionized water, hydrochloric acid, glacial acetic acid, ammonium hydroxide and acetone were purchased from Merck chemicals India.

Measurements and Instruments: Fourier transform-infrared spectra of the samples were recorded by Shimadzu IR Affinity 1 spectrometer using KBr pellet method. Raman spectra of samples were taken in powder form by LabRam spectrometer by HORIBA JOBIN YVON using argon ion laser of wavelength 514.5 nm. UV–Visible spectra of the samples were recorded by Shimadzu UV–Visible spectrophotometer, UV 1800 series in the range of 200–800 nm with HPLC grade chloroform, ethanol and deionized water. The elemental analysis (CHNS) of the samples were recorded by elementar vario EL III element analyzer. The powder wide angle X-ray diffraction of the samples were measured using PANALYTICAL, Aeris research with 2θ values ranging from 3 to 80°. Field emission scanning electron microscopic images were recorded by ZEISS ΣIGMA™ field emission scanning electron microscope (FE-SEM). The transmission electron microscopic analysis was carried out by JOEL/JEM 2100 instrument having capacity of 200 KV with magnification 2000X – 1500000X. Thermogravimetric analysis (TGA) of the samples were measured using PerkinElmer, Diamond TG/DTA in an inert atmosphere of nitrogen at heating rate 20°C/min. The four probe electrical conductivity of the samples was measured using DFP-RM-200 with constant current source Model CCS-01 and DC microvoltmeter. The pH measurements were carried out using HM digital PH -80 Temp hydro tester. XPS analysis has been carried out using PHI 5000 Versa Probe III instrument. Both wide scan spectra (in the range of 150–600 eV) and narrow scan spectra of individual element range were carried out using XPS spectra.

3. General procedure

3.1. Synthesis of MWCNT-COOH

MWCNT (0.40 g) was added to nitric acid (5 M, 50 mL) taken in an R. B. flask and then sonicated for 15 min for making dispersion. The reaction mixture was refluxed at 100 °C for 7 h with magnetic stirring. The refluxed reaction mixture was washed with deionized water until pH of filtrate becomes neutral. It is then washed with acetone, filtered and dried in vacuum oven at 60 °C for 3 h. Yield: 0.36 g. FT-IR (KBr, cm^{-1}) 1465, 1504, 1648, 1698, 1741.

3.2. Synthesis of PTCNT-COOH 300

Thiophene (1 mL, 12.50 mmol) and AOT (0.22 g, 0.50 mmol) was dissolved in chloroform (20 mL) and sonicated for 5 min. To the monomer-AOT mixture, **MWCNT-COOH** (0.30 g) was added and sonicated for 10 min. Ferric chloride (2.43 g, 15.00 mmol) dispersed in 10 mL chloroform was added drop by drop to monomer-surfactant-MWCNT-COOH mixture and sonicated for 15 min. After that it was stirred using a magnetic stirrer for 3 h. The resulting conducting polymer-carbon nanotube composite was washed using water and acetone and dried in vacuum oven at 70 °C for 3 h. Yield: 0.70 g. FT-IR (KBr, cm^{-1}) 675, 785, 1458, 1512, 1648, 1676, 1747. Elemental analysis (anal. wt %) C: 66.58, S: 17.53, H: 0.30.

The nanocomposites **PTCNT-COOH 100** and **PTCNT-COOH 200** were prepared similarly by changing the weight of functionalized **MWCNT** as 0.10 g and 0.20 g respectively (see supporting information for synthesis).

3.3. Synthesis of PTCNT-COOH 300 Ag

The sample **PTCNT-COOH 300** (0.16 g) was dispersed in 500 mL of deionized water by sonication. Ascorbic acid (8.81 g, 5.00 mmol) was added to the above binary composite followed by addition of NaOH solution (10 M, 20 mL, 21.00 mmol) with magnetic stirring for 5 min and allowed to equilibrate the pH for 3 h. Fresh $AgNO_3$ solution (5 mL, 0.30 M, 1.50 mmol) was then added to this mixture under strong stirring condition for 30 s followed by gentle stirring for 30 min at room temperature. The mixture was kept undisturbed for 12 h and after that

washed with deionized water (till pH of filtrate becomes neutral from alkaline). Ternary nanocomposite mixture was finally washed with acetone and dried in vacuum oven at 70 °C for 3 h. Yield: 0.28 g. FT-IR (KBr, cm^{-1}) 693, 787, 1534, 1646, 1695, and 1747.

3.4. Synthesis of MWCNT-COOH Ag

MWCNT-COOH (0.16 g) was dispersed in 500 mL of deionized water by sonication. Ascorbic acid (8.81 g, 5.00 mmol) was added to the above dispersion followed by addition of NaOH solution (10 M, 20 mL, 21.00 mmol) with magnetic stirring for 5 min and allowed to equilibrate the pH for 3 h. Fresh $AgNO_3$ solution (5 mL, 0.30 M, 1.50 mmol) was then added to this mixture under strong stirring condition for 30 s followed by gentle stirring for 30 min at room temperature. The mixture was kept undisturbed for 12 h and after that washed with deionized water (till pH of filtrate becomes neutral from alkaline). Binary silver nanocomposite mixture was finally washed with acetone and dried in vacuum oven at 70 °C. Yield: 0.31 g. FT-IR (KBr, cm^{-1}) 1550, 1646, 1705, 1754.

4. Results and discussions

Polythiophene–functionalized multiwalled carbon nanotube nanocomposites were prepared by *in situ* chemical oxidative polymerization of thiophene monomer in presence of functionalized multiwalled carbon nanotubes (**MWCNT-COOH**) using ferric chloride as the oxidizing agent and sodium bis(2-ethylhexyl) sulfosuccinate (AOT) as anionic surfactant (see Fig. 1). Thiophene-AOT micellar complexes, in the vicinity of functionalized multiwalled carbon nanotubes, get attached to the walls of multiwalled carbon nanotube through non-covalent interactions and get polymerized by oxidizing agents to result water dispersible core shell nanostructured polythiophene-functionalized MWCNT nanocomposites [40]. Multiwalled carbon nanotubes were functionalized by refluxing with nitric acid (5 M) at 100 °C for 7 h. The functionalization of multiwalled carbon nanotube enhances the dispersibility in various polar solvents which in turn facilitates the polymerization of thiophene to takes place easily on the surface of multiwalled carbon nanotubes. For the typical preparation of polythiophene-functionalized multiwalled carbon nanotube nanocomposites, thiophene monomer along with anionic surfactant AOT was dissolved in chloroform followed by the addition of functionalized multiwalled carbon nanotube with sonication (see Table S1 in supporting information). The ferric chloride dispersed in chloroform was added drop by drop to the above mixture for polymerization reaction to take place. The anionic surfactant sodium bis-(2-ethylhexyl) sulfosuccinate was utilized as dopant for polythiophene and stabilizer for polythiophene-functionalized multiwalled carbon nanotube nanocomposites [45–49]. The polymer attached on the surface of functionalized multiwalled carbon nanotube possess more than one non covalent interactions such as pi-pi stacking, weak hydrogen bonding and van der Waals interaction at various positions to stabilize the nanocomposites [50–52].

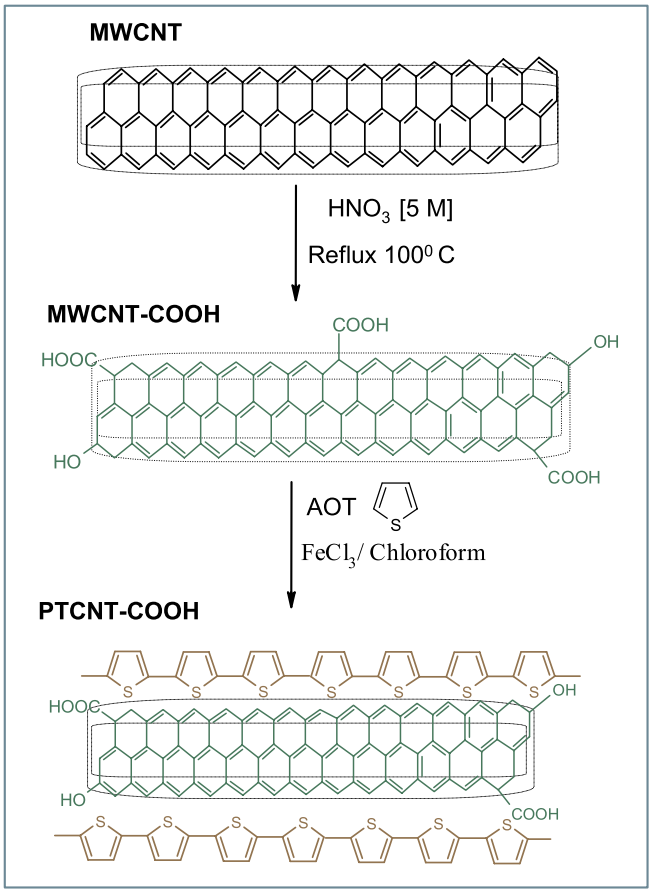

Fig. 1. Schematic representations of synthesis of **MWCNT-COOH** and **PTCNT-COOH**.

The FT-IR spectroscopic studies of the pristine **MWCNT**, **MWCNT-COOH** and **PTCNT-COOHs (100, 200 and 300)** were carried out by making thin pellet of the samples with KBr powder (see Fig. 2). Pristine **MWCNT** have shown characteristic peaks at 1528 and 1641 cm^{-1} due to in-plane vibrations of graphitic walls of carbon nanotubes and C═C stretching vibrations of carbon nanotubes respectively [53–55]. Good symmetry of the carbon nanotube produces weak dipole moment change and hence poor signals [56]. However, functionalized multiwalled carbon nanotubes **MWCNT-COOH** and **PTCNT-COOHs** (**100**, **200** and **300**) have shown strong infrared signals. Functionalized **MWCNT-COOH** samples have shown peaks at 1465, 1504, 1648, 1698 and 1741 cm^{-1} due to C–O bending of aliphatic alcohol, in-plane vibrations of graphitic walls, C═C stretching vibrations, C═O stretching vibrations of carbonyl (keto or aldehyde functional group) and C=O streching vibration of carboxylic groups respectively [53–59]. **PTCNT-COOHs** nanocomposites (**100**, **200** and **300**) have two extra peaks present at 785 and 675 cm^{-1} corresponding to C–H out of plane deformation and C–S stretching of polythiophene chains in addition to the peaks in **MWCNT-COOH** [26,60–62]. FT-IR spectra of polythiophene was shown in supporting Fig. S1. The broad peaks were present in the range 3612–3744 cm^{-1} belongs to hydrogen bonded OH functional groups including water molecules attached to CNT (see supporting Fig. S2) [63, 64]. Raman spectroscopy of purified **MWCNT** (see supporting information) and functionalized **MWCNT-COOH** have been carried out to find out the extent of disorder in the graphitic structure of multiwalled

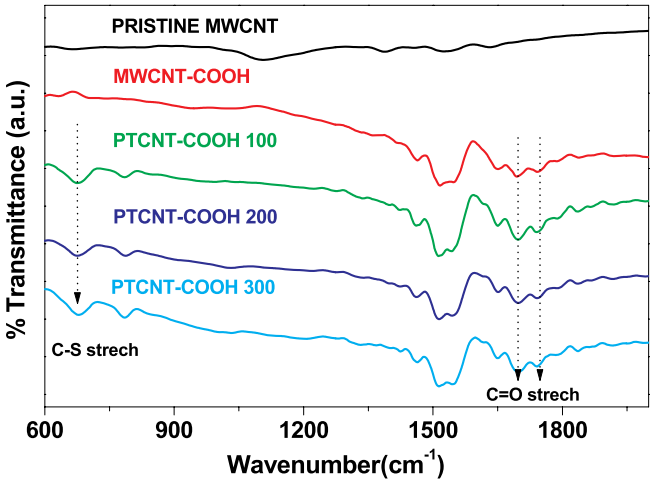

Fig. 2. FT-IR Spectra of pristine **MWCNT**, **MWCNT-COOH**, **PTCNT-COOH 100**, **PTCNT-COOH 200** and **PTCNT-COOH 300**.

carbon nanotube (see supporting Fig. S3). The characteristic peaks of multiwalled carbon nanotube termed as G band for graphitic structure and D-band for disorder and defects of structure were present at 1576 cm^{-1} and 1348 cm^{-1} respectively [54,56,63]. The G band was due to in-plane tangential stretching of the carbon-carbon bonds in graphene sheets and D band is due to presence of amorphous carbon and disordered structure in CNT [56,65,66]. The I_D/I_G ratio of purified **MWCNT** and functionalized **MWCNT-COOH** were found to be 1.28 and 1.34 respectively. The acid washing removes the impurities, however acid oxidation produced functionalization of carbon nanotube as well as removal of impurities which gives higher the I_D/I_G ratio for functionalized **MWCNT-COOH** [54,67,68].

The X-ray photoelectron spectroscopy (XPS) analysis of pristine **MWCNT**, functionalized **MWCNT-COOH**, **PTCNT-COOH 100** and **PTCNT-COOH 300** has been carried out to understand their functionalization ratio (see Fig. 3 and see Table 1). Pristine **MWCNT** have shown high intensity peak at 283.25 and very weak intensity peak at 531.45 eV corresponding to C 1s and O 1s respectively. **MWCNT-COOH** exhibited intense peak at 283.45 corresponding to C 1s and relatively intense peak at 531.6 eV corresponding to O 1s (see Fig. 3) [65]. An enhancement in the intensity of O 1s peak was observed in functionalized **MWCNT-COOH** in comparison with pristine **MWCNT,** which reveals that oxygen containing functional groups were incorporated by acid oxidation. Samples like **PTCNT-COOH 100** and **PTCNT-COOH 300** were exhibited characteristic peaks of sulfur at 226.95 eV (S 2s) and 162.75 eV (S 2p) in addition to C 1s and O 1s peaks, which confirms the presence of polythiophene in **PTCNT-COOHs** [22,69]. Nanocomposite samples like **PTCNT-COOH 100** contains high compositional ratio of polythiophene, which was evident from its higher peak intensity than **PTCNT-COOH 300**. The pH measurements of the samples like **MWCNT-COOH**, **PTCNT-COOH 100**, **PTCNT-COOH 200** and **PTCNT-COOH 300** have been carried out by dispersing samples in water via sonication. The pH measurement of **MWCNT-COOH** have shown pH value 4.8 (acidic due to dissociation of H^+ ion from carboxylic acid groups present), whereas pH values of **PTCNT-COOH 300**, **PTCNT-COOH 200, PTCNT-COOH 100** were gradually increased to 5.4, 6.2 and 6.7 respectively. **MWCNT-COOH** was relatively more acidic due to carboxylic acid groups, whereas in nanocomposites of **PTCNT-COOHs** gradually lose acidity as we decrease the amount of MWCNT-COOH in feed. The decrease in acidity was not due to suppression of dissociation of the hydrogen ions by the polythiophene layer, but due to low amount of **MWCNT-COOH** added to the system.

The solid state ordering of functionalized **MWCNT-COOH**, polythiophene (**PT**), **PTCNT-COOH 100, PTCNT-COOH 200** and **PTCNT-COOH 300** have been analyzed by powder X-ray diffraction studies (see Fig. 4). Functionalized **MWCNT-COOH** have shown mainly an intense peak at 2θ value 25.85° due to (002) diffraction plane of **MWCNT** with a graphitic structure [70–72] (See supporting Fig. S4 for WXRD of pristine **MWCNT**). Polythiophene (**PT**) has the amorphous broad peak centered at 18.68°. Polythiophene-functionalized multiwalled carbon nanotube nanocomposites like **PTCNT-COOH 100, PTCNT-COOH 200** and **PTCNT-COOH 300** were also shown (002) peaks of carbon nanotube at 2θ value 26.02°. The intensity of (002) peak goes up and the intensity of amorphous peak of polythiophene (in the 2θ range 13–30°) goes down on moving from **PTCNT-COOH 100** to **PTCNT-COOH 300**. This result suggests that polythiophene was attached as nano-layer to PTC**NT-COOH 300**, which have more surface area than other samples [73–75]. The low compositional ratio of thiophene in **PTCNT-COOH 300** was reversed by increasing the thiophene monomer in feed (see supporting information for the synthesis **PT2CNT-COOH 300 and PT3CNT-COOH 300**). On increasing the thiophene content in feed, amorphous peak of polythiophene increases (see supporting Fig. S5). Powder X-ray diffraction studies have revealed that ordered arrangement of polythiophene increases with the more surface area of multiwalled carbon nanotubes. Weak non-covalent forces like π-π stacking, hydrogen bonding and van der Waal forces present in the nanocomposites assist the formation of ordered solid state packing in polymer-carbon nanocomposites.

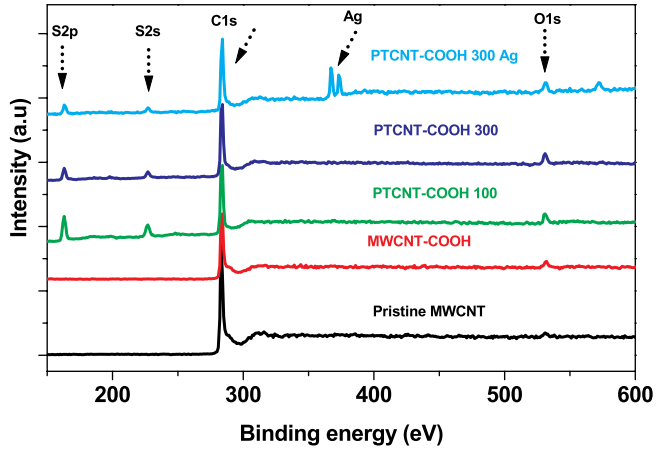

Fig. 3. XPS spectra of pristine **MWCNT**, functionalized **MWCNT-COOH, PTCNT-COOH-100, PTCNT-COOH 300 and PTCNT-COOH 300 Ag**.

The surface features and shape of functionalized **MWCNT-COOH** and **PTCNT-COOHs** (100 and 300) were analyzed using scanning electron microscopy (see Fig. 5). Field emission-scanning electron microscopy images of pristine **MWCNT** have bundled nature (see supporting Fig. S6), whereas acid functionalization in **MWCNT-COOH** produces cleanly separated carbon nanotubes as a result of purification and washing. Therefore, functionalized carbon nanotube (**MWCNT-COOH**) utilized in the present case could easily retain the nanotube core structure without cut shorted length for the formation of nanocomposites with polythiophene. However, binary nanocomposites such as **PTCNT-COOHs (100 and 300)** have shown an increase in thickness without any phase separation. The inner dimensions of the nanocomposite (**PTCNT-COOH 300**) have been analyzed using transmission electron microscopy (TEM) (see Fig. 5 d). TEM images have shown comparably thick outer layer with outer diameter of 14.80 ± 5 nm and inner tube diameter of 4.20 ± 3 nm (see supporting Fig. S7). Higher diameter ratio (outer/inner) suggests that polythiophene was attached on the surface of the MWCNT as an outer layer through weak non-covalent interactions, which was responsible for the core shell morphology formation reported similar to our previous work [40].

The pristine multiwalled carbon nanotubes were usually insoluble in any common solvents mainly due to bundling nature of carbon nanotubes and lack of functionalization. However, covalent functionalization of multiwalled carbon nanotube by acid oxidation introduces polar groups such as carboxylic acid, hydroxyl and carbonyl groups which enhance the solubility, especially in polar solvents. The functionalized **MWCNT-COOH** covered with conducting polymers reduces the bundling effect via repulsion between the tethered polymer chains creating an energy barrier against aggregation by controlling intertube potential [74]. Theoretical aspects with simulation study based on interaction of conducting polymers with carbon nanotubes utilizing non-covalent interactions could enhance better performance in dispersibility and hence the processability [75]. Sonication of functionalized **MWCNT-COOH** and **PTCNT-COOHs** (100, 200 and 300) nanocomposites in water, ethanol and chloroform have produced fairly stable dispersions (see supporting Fig. S8). The functionalized multiwalled carbon nanotube (**MWCNT-COOH**) have shown absorption maximum at 260 nm due to aromatic π-π* absorption of carbon nanotube (see supporting Fig. S9) [76,77]. The UV–visible spectra of **PTCNT-COOH 100** in chloroform and **PTCNT-COOH 300** in ethanol and chloroform have shown well resolved peak at 360 nm in addition to peak at 280 nm (see Fig. 6). The characteristic peak at 360 nm was due to π-polaron transition of polythiophene, which was intense for **PTCNT-COOH 100**. The sample **PTCNT-COOH 100** possess less amount

Table 1
Atomic concentration of samples from XPS spectra, pH of the samples, morphology of samples, thermal stability of samples, and electrical conductivity of samples.

Samples	Components	Type of nanocomposite	Atomic Concentration (%)				pH	Shape	Thermal Stability (°C)	Conductivity (S/cm)
			C1s	O2s	S2p	Ag3d				
Pristine MWCNT	–	–	98.36	1.64	–	–	–	nanotubes	–	8.66
MWCNT-COOH	–	–	94.42	5.58	–	–	4.8	nanotubes	560	2.80
PTCNT-COOH 100	Thiophene + MWCNT-COOH	Binary	82.44	5.63	11.93	–	6.7	PT covered nanotubes	300	0.04
PTCNT-COOH-200	Thiophene + MWCNT-COOH	Binary	–	–	–	–	6.2	PT covered Nanotubes	-	0.53
PTCNT-COOH-300	Thiophene + MWCNT-COOH	Binary	88.63	5.70	5.68	–	5.4	PT covered Nanotubes	340	1.64
MWCNT-COOH Ag	MWCNT-COOH + Ag	Binary	–	–	–	–		Ag Nanoparticles + nanotubes	750	12.40
PTCNT-COOH 300 Ag	Thiophene + Ag + MWCNT-COOH	Ternary	86.66	7.75	4.22	2.37	7.9	Ag Nanoparticles + PT covered Nanotubes	620	80.76

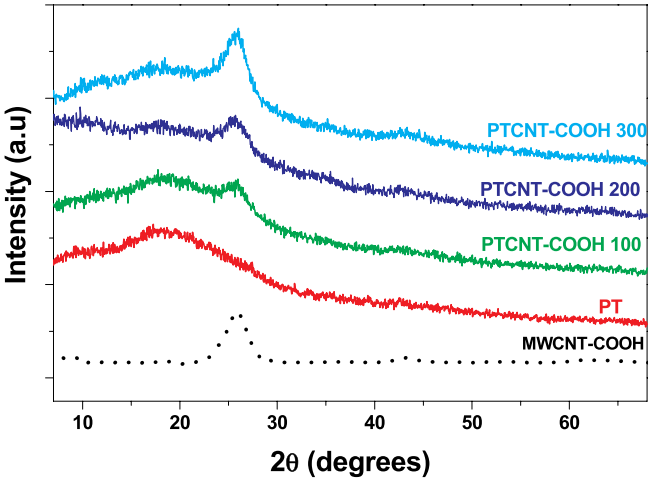

Fig. 4. Wide angle powder X-ray diffraction patterns of **MWCNT-COOH,** Polythiophene **(PT), PTCNT-COOH 100, PTCNT-COOH 200 and PTCNT-COOH 300.**

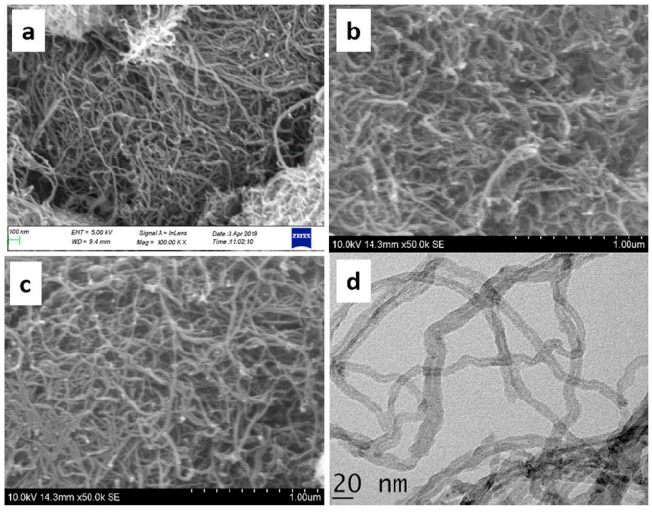

Fig. 5. FE-SEM images of a) functionalized **MWCNT-COOH,** b) **PTCNT-COOH 100**, c) **PTCNT-COOH 300** and d) High resolution TEM image of **PTCNT-COOH 300.**

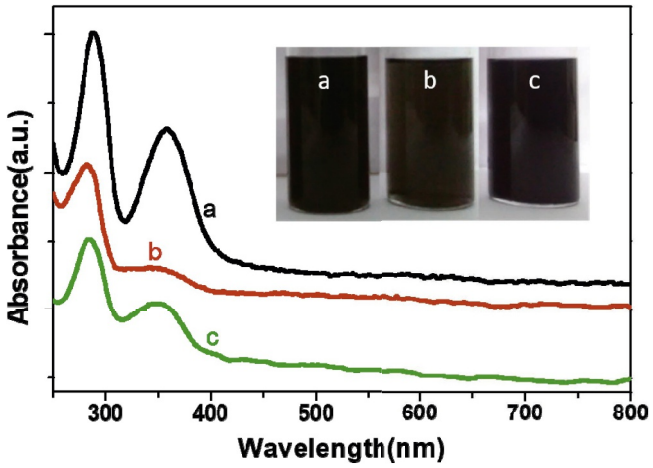

Fig. 6. UV–visible absorption spectra of a) **PTCNT-COOH 100** in chloroform, b) **PTCNT-COOH 300** in chloroform and c) **PTCNT-COOH 300** in ethanol.

of functionalized **MWCNT-COOH** (100 mg) than **PTCNT-COOH 300** (300 mg), therefore thick layer present in **PTCNT-COOH 100** must have resulted in strong absorption of polaron transition (see Fig. 6) [25,39].

In the present system, we have obtained stable nanodispersion by sonicating polythiophene-multiwalled carbon nanotubes in water and ethanol, which was advantageous for making higher order (ternary or quaternary) nanocomposites. Here, we have attempted to synthesize silver nanoparticles embedded polythiophene-multiwalled carbon nanotube ternary nanocomposites by making use of its dispersibility in water. Polythiophene-functionalized multiwalled carbon nanotube nanocomposite system can act as effective host for accommodating silver nanoparticle and to act as a stabilizer to prevent bulk aggregation of silver nanoparticles into microns. The ternary nanocomposite **PTCNT-COOH 300 Ag** was prepared by reducing aqueous silver nitrate solution into silver nanoparticles using ascorbic acid as the reducing agent in presence of water dispersed **PTCNT-COOH 300** nanocomposites (see supporting Fig. S10). A similar method was also used to synthesize binary silver nanocomposite with functionalized **MWCNT-COOH** (no conducting polymer) represented as **MWCNT-COOH Ag**. **PTCNT-COOH 300 Ag** and **MWCNT-COOH Ag** were subjected to FT-IR studies in order to characterize the formation of respective nanocomposites (see Fig. 7A). The functionalized **MWCNT-COOH Ag** have shown peaks at 1550 cm^{-1}, 1646 cm^{-1}, 1695 cm^{-1} and 1747 cm^{-1} corresponding to in-plane vibrations of graphitic walls, C═C stretching vibrations, carbonyl groups and C═O stretching vibrations in acid groups respectively. **PTCNT-COOH 300 Ag** sample have shown characteristic peaks of thiophene at 787 cm^{-1} and 693 cm^{-1} due to C–H out-of-plane

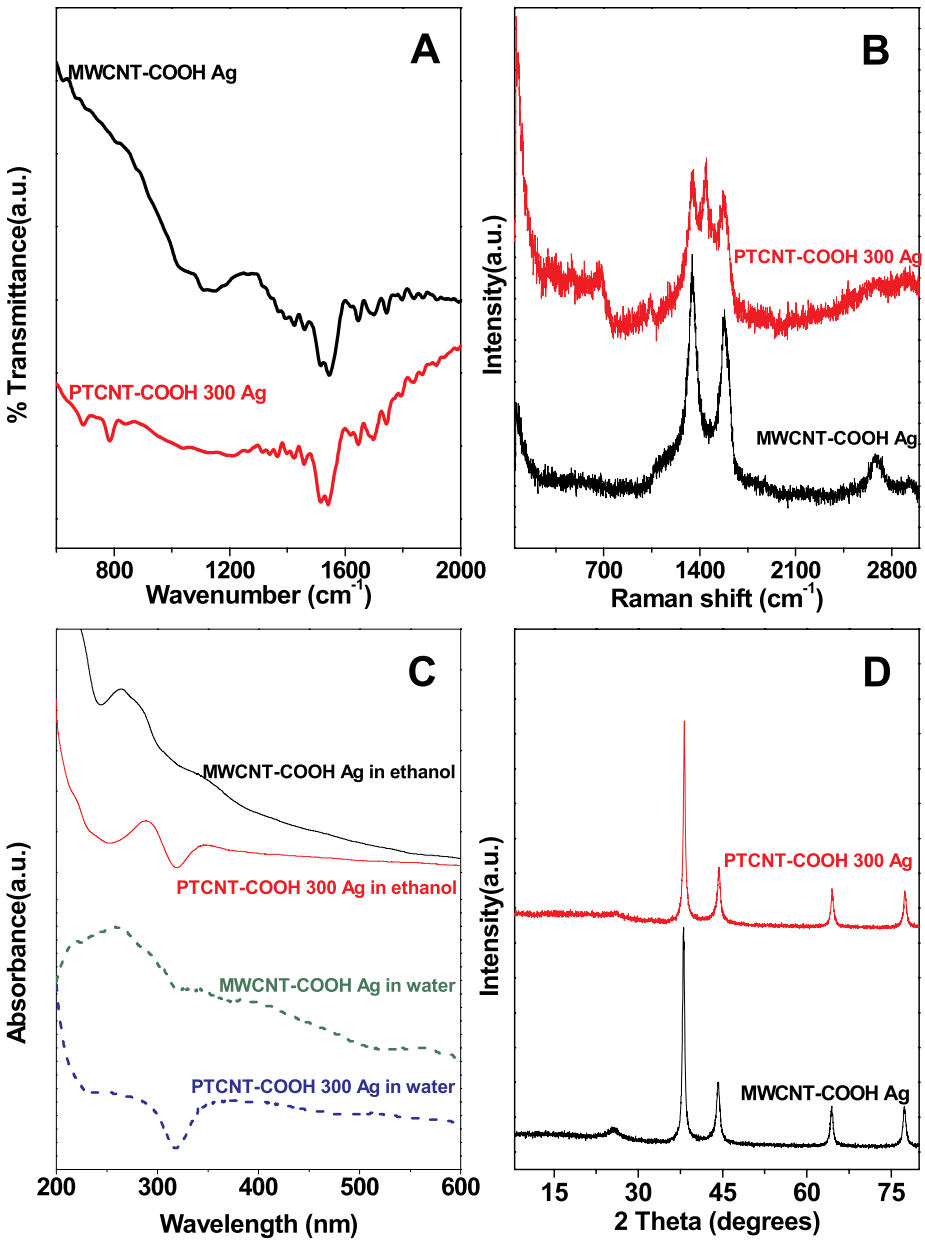

Fig. 7. (A) FT-IR Spectra of **MWCNT-COOH Ag** and **PTCNT-COOH 300 Ag**, (B) Raman spectra of **MWCNT-COOH Ag** and **PTCNT-COOH 300 Ag**, (C) UV–Visible spectra of **MWCNT-COOH Ag** and **PTCNT-COOH 300 Ag** in water and ethanol and (D) Wide angle XRD pattern of **MWCNT-COOH Ag** and **PTCNT-COOH 300 Ag.**

deformation mode and C–S stretching mode of thiophene ring in addition to functionalized **MWCNT-COOH** peaks. **PTCNT-COOH 300 Ag** sample have shown decline in carbonyl stretching frequency at 1695 and 1747 cm^{-1} and the C–S stretching frequency at 693 cm^{-1} which could be attributed to the ternary nanocomposite formation with silver [72,78]. FT-Raman spectra of **PTCNT-COOH 300 Ag** and **MWCNT-COOH Ag** in powder form were recorded using 514.5 nm argon laser (see Fig. 7B). **MWCNT-COOH Ag** has shown characteristic G band and D band at 1576 cm^{-1} and 1348 cm^{-1} respectively. In the case of **PTCNT-COOH 300 Ag**, an additional intense peak was observed at 1450 cm^{-1} due to symmetric in phase vibration of polythiophene chain, which confirms the presence of polythiophene in these ternary nanocomposite [43a,79, 80]. **MWCNT-COOH Ag** and **PTCNT-COOH 300 Ag** were easily dispersed in water and ethanol which enabled us to record the UV–visible absorption spectra (see Fig. 7C and supporting Fig. S11 for dispersions). Tendency of formation of stable dispersions was retained in ternary composite by keeping energy barrier against aggregation. The UV–visible absorption spectra have shown absorption maxima at 285 nm, which was due to the absorption from multiwalled carbon nanotube. The ternary nanocomposite **PTCNT-COOH 300 Ag** sample in water and ethanol have shown π-polaron peak at 360 nm. Surprisingly, the longer wavelength peak at 360 nm was extended as shoulder up to 550 nm, which could be attributed to the surface plasmon resonance of silver nanoparticles [81,82]. Wide angle X-ray diffraction studies of **PTCNT-COOH Ag** and **MWCNT-COOH Ag** have been carried out to confirm the formation of silver nanoparticles in conducting polythiophene-functionalized MWCNT nanocomposite (see Fig. 7D). Both the samples have shown highly crystalline peaks at 2θ values 38.15°, 44.33°, 64.52°and 77.46°, which represent Bragg's reflections from (111), (200), (220) and (311) planes of Ag nanoparticles in nanocomposite [83]. The weak peak at 2θ value 26.69° was due to diffraction from (002) plane of the graphitic structure of CNT. The presence of highly crystalline silver nanoparticles increases the overall solid state ordering of the samples [50,84]. The XPS spectra of

PTCNT-COOH 300 Ag have shown peaks of silver atoms present at 367.45 and 373.45 eV representing binding energies of $3d_{5/2}$ and $3d_{3/2}$ respectively which indicates the formation of silver nanoparticles in the nanocomposite (see Fig. 3) [85].

The field emission scanning electron microscopic images of **PTCNT-COOH 300 Ag** and **PTCNT-COOH 300 Ag** dispersed in acetone have exhibited silver nanoparticles embedded on polythiophene-functionalized multiwalled carbon nanotube nanocomposite (see Fig. 8a and b respectively). The striking observation made from field emission-scanning electron microscopy images of **PTCNT-COOH 300 Ag** (Fig. 8a) was that embedded silver nanoparticles show the tangled nature (rather than straight) and also have spaces between each nanotube of ternary nanocomposites. The predominant involvement of non-covalent interaction of **PTCNT-COOH 300** with silver nanoparticles was evident from these images. Otherwise, severe bulk aggregation would have resulted between mutually attached nanotubes by silver coating (See supporting Fig. S12). The field emission scanning electron microscopic images of **MWCNT-COOH Ag**, binary composite without polymer have shown a mix of multiwalled carbon nanotubes and silver nanoparticles with slightly higher size 40 ± 10 nm in the composite matrix. Thiophene layer that predominantly control the decoration of the silver nanoparticles rather than limited acid functionalized groups attached to the functionalized multiwalled carbon nanotube. Transmission electron microscopic analysis of the nanoparticles have revealed that the formation of tangled solid silver nanoparticles over **PTCNT-COOH** nanocomposites with average size 25 ± 8 nm by taking average of 10–12 nanoparticles (see Fig. 8 d). Entangled silver nanoparticles embedded over polythiophene-multiwalled carbon nanotube appears as aggregated silver particles. However, there were isolated nanoparticles in the **PTCNT-COOH** fibrous matrix (see supporting Fig. S13) and a close look on the silver nanoparticles revealed they were embedded to the nanocomposites matrix. **PTCNT-COOH 300 Ag** has ring like electron diffraction pattern with bright spots, which indicates that Ag nanoparticles were crystalline in nature (see supporting Fig. S14) [86]. It is important to note that silver nanoparticles have nearly spherical shape even they exist as tangled condition. In the case of ternary silver nanocomposite formation, the Ag^{+} ions from silver nitrate were attracted to sulfur atom in the heterocyclic polythiophene chains and get reduced to silver nanoparticles by accepting electrons from ascorbic acid present in the aqueous dispersion. Ascorbic acid itself converted to radical ion semidehydroascorbic acid and then to dehydroascorbic acid [85,87,88]. Silver nanoparticles formed were anchored to the surface of **PTCNT-COOH 300** matrix through the complex formation of silver atoms with sulfur atoms of polythiophene chains and carboxylate group of functionalized multiwalled carbon nanotube [43a,82]. The sulfur atoms in closely packed polythiophene chains can assist the silver nanoparticles to decorate over the **PTCNT-COOH** in a tangling fashion along with carboxylic acid group of functionalized carbon nanotubes using the non-covalent force of interactions (see the scheme Fig. 9).

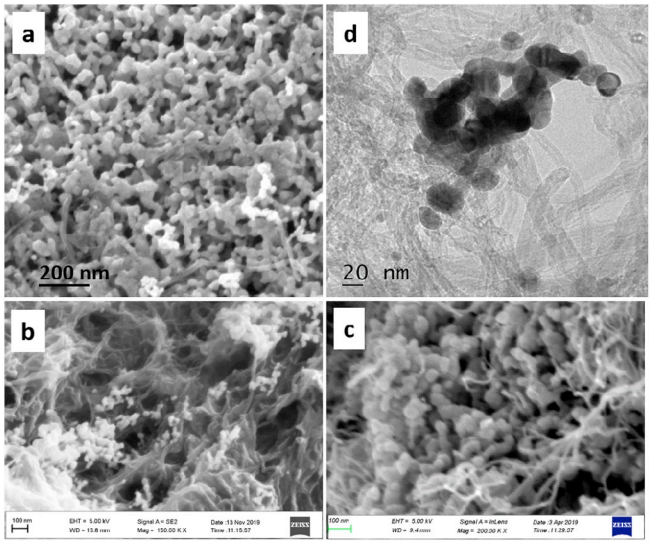

Fig. 8. Field emission scanning electron microscopy images of (a) **PTCNT-COOH 300 Ag** (b) dispersed **PTCNT-COOH 300 Ag** in acetone (c) **MWCNT-COOH Ag** and (d) Transmission electron microscopy image of **PTCNT-COOH 300 Ag**.

The four probe electrical conductivity of the samples were recorded by DFP-RM-200 four probe set-up with constant current. The electrical conductivity of the samples were measured at four different points and average value has been reported. The electrical conductivity of the polythiophene (**PT**), **PTCNT-COOH 100, PTCNT-COOH 200**, **PTCNT-COOH 300**, **pristine MWCNT,** functionalized **MWCNT-COOH, MWCNT-COOH Ag** and **PTCNT-COOH 300 Ag** were 4.42×10^{-2}, 5.30×10^{-1}, 1.64, 8.66, 2.80, 12.40 and 80.76 S/cm respectively (see Fig. 10). The electrical conductivity of polythiophene was less than pristine multiwalled carbon nanotube and polythiophene-functionalized multiwalled carbon binary nanocomposites [89]. Effective charge transfer of the charge carriers in binary and ternary nanocomposites resulted in higher electrical conductivity. Literature studies reveals that electrical conductivity of polythiophene have reported both in the semiconducting and conducting range [26,61]. However, polythiophene derivatives like poly(3,4-ethylenedioxy thiophene), poly(3,4-dimethyl thiophene), shows higher conductivity by pinning of charges with appropriate methods [90,91]. Decreased band gap due to proper conductive pathways for carrier mobility and stable doped state in the polymeric material would result in good conductive nature to the conjugated polymer. The silver nanoparticles loaded polythiophene-functionalized MWCNT nanocomposites were an interesting case of ternary conducting polymer nanocomposites, because the conducting polythiophene layer can act as conductive bridge which may help to transfer electrical charge between more conducting silver and multiwalled carbon nanotube via hopping mechanism and hence it can increase the overall electrical conductivity of the system.

Thermal stability of functionalized **MWCNT-COOH, PTCNT-COOH 100, PTCNT-COOH 300, MWCNT-COOH Ag** and **PTCNT-COOH 300 Ag** have been carried out using thermogravimetric analysis at a heating rate of 20°C per minute under inert nitrogen atmosphere (see Fig. 11). The samples **PTCNT-COOH**s (100 and 300) have shown 10% weight loss at 300 °C. Samples like functionalized **MWCNT-COOH** and **PTCNT-COOH 300 Ag** have shown 10% weight loss at 620 °C. Accommodation of silver nanoparticles in ternary composite **PTCNT-COOH 300 Ag** enhances the thermal conductivity of the system [92,93]. The high thermal conductivity of multiwalled carbon nanotube and silver nanoparticles might have played a crucial role to enhance thermal stability by building a perfect heat transfer network in ternary nanocomposite even though it contain high percentage of thermally less stable polythiophene [93,94]. The highest thermal stability obtained for **MWCNT-COOH Ag** for 10% weight loss was 750 °C, which was devoid of any polymer sample. Therefore, the thermal stability of **PTCNT-COOH** (binary composite) and functionalized **MWCNT-COOH** could be increased significantly by making tangled sliver nanoparticle nanocomposites [95] (see supporting Fig. S15 for DTG). Relatively poor thermal stability of the conducting **PTCNT-COOH** nanocomposites was due to the degradation of carbon from polythiophene chains and also low content of multiwalled carbon nanotubes for their preparation [40]. The pH sensitivity of the ternary nanocomposite system has been checked by the leaching tendency of embedded silver in ternary nanocomposite in acidic, basic and neutral medium (see supporting information for procedure and supporting Fig. S16). Stability of the ternary nanocomposite at different pH has been checked via UV–visible absorption spectroscopy by noting the changes of surface plasmon peak (>360 nm). The study revealed that silver nanoparticles have good stability against leaching in basic medium (high pH). Ternary nanocomposites can be effectively utilized for

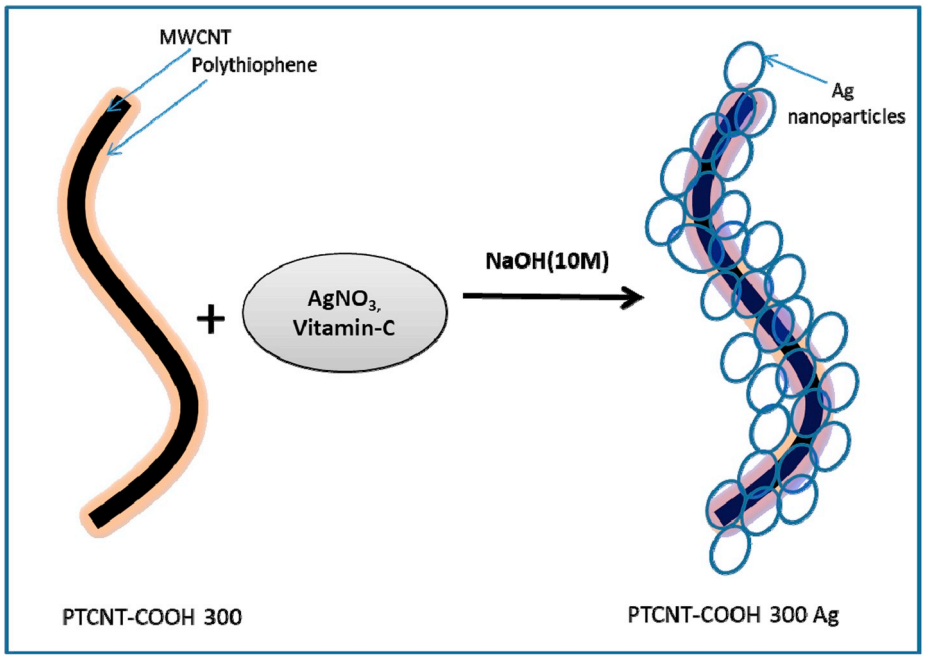

Fig. 9. Schematic representation of formation of silver embedded ternary nanocomposite.

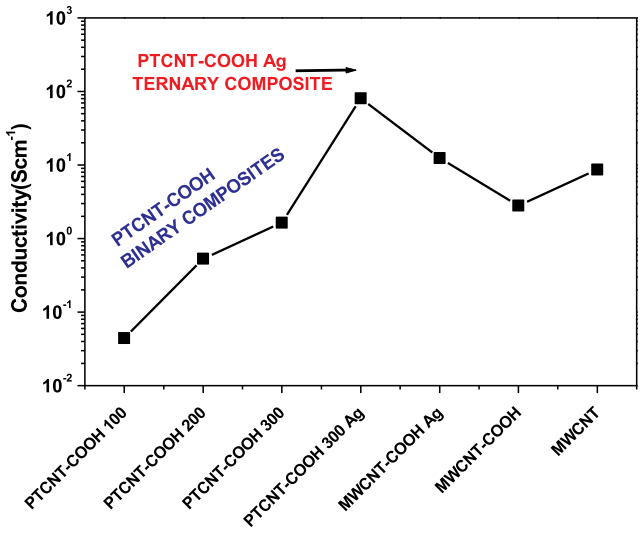

Fig. 10. Four probe electrical conductivity measurements of pristine **MWCNT**, **PTCNT- COOH 100**, **PTCNT-COOH 200**, **PTCNT-COOH 300**, **MWCNT-COOH Ag** and **PTCNT-COOH 300 Ag**.

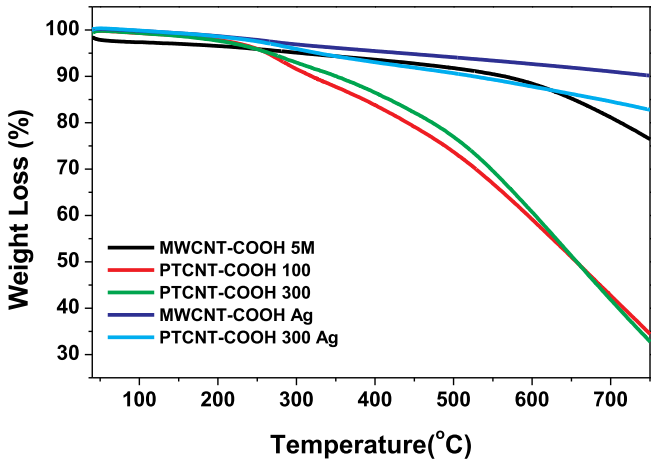

Fig. 11. Thermogravimetric analysis of **MWCNT-COOH**, **PTCNT-COOH 100**, **PTCNT-COOH 300**, **MWCNT-COOH Ag** and **PTCNT-COOH 300 Ag**.

catalytic applications in a basic medium and therefore it can be durable catalyst with multiple use [96,97]. Literature studies reveal that the present work has significant advantages over other nano composite systems especially in cost, efficiency and many other deserving merits related to conductivity and thermal stability (see Table S2 in supporting information). Synthesis of tangled silver nanoparticles embedded on polythiophene-functionalized multiwalled carbon nanotube has been adopted in cheapest and greener medium. The binary and ternary composites have been prepared efficiently in a laboratory scale with reproducibility and the processability of the nanocomposites as stable dispersion in water and ethanol has been accomplished. Ternary nanocomposite could also perform well in suitable high temperature applications due to its high thermal stability. By comparing with other systems we could observe that mutually connected nanoparticles exhibited good performance in different applications. Easy synthesis, remarkable electrical conductivity, good solid state ordering and thermal stability of ternary nanocomposites can open doorway to different applications such as high performance electrochemical electrodes, polymer super capacitors, sensors, SERS tags, thermoelectric materials, catalytic applications and so on.

5. Conclusion

In summary, the present work demonstrated a facile and green synthetic approach to prepare water dispersible, highly conductive and thermally stable ternary silver nanoparticles embedded polythiophene-functionalized multiwalled carbon nanotube nanocomposite (**PTCNT-COOH 300 Ag**) by efficiently utilizing the aqueous dispersion of binary polythiophene-functionalized multiwalled carbon nanotube nanocomposite (**PTCNT-COOH**) as a nanofibrous platform as well as co-component matrix in its ternary nanocomposite. Here we could effectively establish facile synthesis of **PTCNT-COOH 300 Ag** from dispersed

state of **PTCNT-COOH** binary composite by reduction of silver nitrate using ascorbic acid in green solvent water. The important outcomes of the present investigations are summarized as follows i) FT-IR spectra of the samples have given primary evidence of nanocomposite formation by examining peaks corresponding to both functionalized MWCNT and polythiophene. ii) Raman spectra have shown that I_D/I_G ratio of purified **MWCNT** and functionalized **MWCNT-COOH** were 1.28 and 1.34 respectively which is comparable to the literature. Raman spectrum of **PTCNT-COOH 300 Ag** has shown the characteristic peaks of polythiophene at 1450 cm^{-1} iii) X-ray photoelectron spectroscopy have shown the corresponding binding energies of each elements present in nanocomposites which confirms functionalization of **MWCNT** and also the formation of binary and ternary nanocomposites. (iv) The pH measurements indicated that acid functionalized multi-walled carbon nanotubes (**MWCNT-COOH**) shows acidic pH due to the presence of free carboxylic acid groups. (v) Powder WXRD studies of binary composites (**PTCNT-COOHs**) have shown amorphous peaks of polythiophene in the range of 13–30° along with peak corresponding to (002) plane of MWCNT at 26.02°. vi) The formation of crystalline silver nanoparticles in **PTCNT-COOH 300 Ag** was confirmed by WXRD analysis by noting the sharp crystalline peaks at 38.15°, 44.33°, 64.52° and 77.46° indicated by Bragg's reflections from (111), (200), (220) and (311) planes. (vii) Scanning and transmission electron microscopic analysis gave information about the formation of thick polymer layer around the outer walls of **MWCNT** and also shows embedded silver nanoparticles with average size 25 ± 8 nm in **PTCNT-COOH 300 Ag.** (viii) UV–Visible spectra of functionalized **MWCNT-COOH** have provided characteristic absorption band at 260 nm characteristic of aromatic π-π* absorption, whereas in **PTCNT-COOHs** (100, 200 and 300) were shown additional band at 360 nm corresponding to π-polaron band of polythiophene. (ix) The nanocomposites **PTCNT-COOH 300 Ag** and **MWCNT-COOH Ag** have shown surface plasmon resonance of silver nanoparticles as shoulder up to 550 nm. (x) Tangled silver nanoparticles formed in the ternary nanocomposites were embedded over polythiophene-functionalized multiwalled carbon nanotube by the complex formation of sulfur atoms of polythiophene with silver. xi) Electrical conductivity of binary nanocomposites **PTCNT-COOH 100, PTCNT-COOH 200** and **PTCNT-COOH 300** were 4.42×10^{-2}, 5.30×10^{-1}, 1.64 S/cm respectively and that of ternary silver nanocomposite **PTCNT-COOH 300 Ag** was 80.76 S/cm. (xii) **PTCNT-COOH 300 Ag** have exhibited higher thermal stability (two times higher) than **PTCNT-COOH** for 10% weight loss due to the presence of embedded silver nanoparticles. In a nut shell, we have put forward a simple and green approach for the synthesis of tangled silver nanoparticles embedded over layered polythiophene-functionalized multiwalled carbon nanotube ternary nanocomposites possessing very good dispersibility in water, high conductivity, good solid state ordering and good thermal stability. The ternary silver nanocomposites **PTCNT-COOH 300 Ag** can be effectively utilized for catalytical, antibacterial, electrical and thermal applications based on its dispersibility, reusability, enhanced electrical conductivity and thermal stability.

Author contribution

T. S. Swathy: Methodology, Investigation, Formal Analysis, Writing Draft.

M. Jinish Antony: Conceptualization, Editing and Supervison.

Declaration of competing interest

The authors declare that they have no known competing financial interests or personal relationships that could have appeared to influence the work reported in this paper.

Acknowledgement

We acknowledge DST for FIST facilities and UGC for CPE funded central instrumentation facilities in St. Thomas College (autonomous), Thrissur. We also acknowledge STIC, Cochin for instrumental facilities availed such as elemental analysis, scanning electron microscopy, transmission electron microscopy, powder X-ray diffraction and thermo gravimetric analysis. We acknowledge Department of Physics, CUSAT, Cochin for providing Raman spectroscopy and FE-SEM facility. We acknowledge IIT-Roorkey for providing XPS experimental support. STS acknowledge university grants commission (UGC), New Delhi for JRF fellowship.

Appendix A. Supplementary data

Supplementary data to this article can be found online at https://doi.org/10.1016/j.polymer.2020.122171.

References

[1] T.A. Skotheim, J.R. Reynolds, Conjugated Polymers, Theory, Synthesis, Properties and Characterization, 2007.
[2] Z. Spitalsky, D. Tasis, K. Papagelis, C. Galiotis, Carbon nanotube–polymer composites: chemistry, processing, mechanical and electrical properties, Prog. Polym. Sci. 35 (2010) 357–401, https://doi.org/10.1016/j.progpolymsci.2009.09.003.
[3] H. Shirakawa, The discovery of polyacetylene film: the dawning of an era of conducting polymers (nobel lecture), Angew. Chem. Int. Ed. 40 (2001) 2574–2580, https://doi.org/10.1002/1521-3773(20010716)40:14<2574::AID-ANIE2574>3.0.CO;2-N.
[4] D.M. Guldi, G.M.A. Rahman, F. Zerbetto, M. Prato, Carbon nanotubes in electron Donor−Acceptor nanocomposites, Acc. Chem. Res. 38 (2005) 871–878, https://doi.org/10.1021/ar040238i.
[5] X. Gong, J. Liu, S. Baskaran, R.D. Voise, J.S. Young, Surfactant-Assisted processing of carbon nanotube/polymer composites, Chem. Mater. 12 (2000) 1049–1052, https://doi.org/10.1021/cm9906396.
[6] C. Gao, G. Chen, Conducting polymer/carbon particle thermoelectric composites: emerging green energy materials, Compos. Sci. Technol. 124 (2016) 52–70, https://doi.org/10.1016/j.compscitech.2016.01.014.
[7] C. Zhan, G. Yu, Y. Lu, L. Wang, E. Wujcik, S. Wei, Conductive polymer nanocomposites: a critical review of modern advanced devices, J. Mater. Chem. C. 5 (2017) 1569–1585, https://doi.org/10.1039/c6tc04269d.
[8] T. Khezri, M. Sharif, B. Pourabas, Polythiophene-graphene oxide doped epoxy resin nanocomposites with enhanced electrical, mechanical and thermal properties, RSC Adv. 6 (2016) 93680–93693, https://doi.org/10.1039/c6ra16701b.
[9] Z. Daşdelen, Y. Yıldız, S. Eriş, F. Şen, Enhanced electrocatalytic activity and durability of Pt nanoparticles decorated on GO-PVP hybride material for methanol oxidation reaction, Appl. Catal. B Environ. 219 (2017) 511–516, https://doi.org/10.1016/j.apcatb.2017.08.014.
[10] S. Eris, Z. Daşdelen, Y. Yıldız, F. Sen, Nanostructured Polyaniline-rGO decorated platinum catalyst with enhanced activity and durability for Methanol oxidation, Int. J. Hydrogen Energy 43 (2018) 1337–1343, https://doi.org/10.1016/j.ijhydene.2017.11.051.
[11] M. Moniruzzaman, K.I. Winey, Polymer nanocomposites containing carbon nanotubes, Macromolecules 39 (2006) 5194–5205, https://doi.org/10.1021/ma060733p.
[12] R.K. Prusty, D.K. Rathore, B.C. Ray, CNT/polymer interface in polymeric composites and its sensitivity study at different environments, Adv. Colloid Interface Sci. 240 (2017) 77–106, https://doi.org/10.1016/j.cis.2016.12.008.
[13] R.D. McCullough, The chemistry of conducting polythiophenes, Adv. Mater. 10 (1998) 93–116, https://doi.org/10.1002/(SICI)1521-4095(199801)10:2<93::AID-ADMA93>3.0.CO;2-F.
[14] S.A. Curran, P.M. Ajayan, W.J. Blau, D.L. Carroll, J.N. Coleman, A.B. Dalton, et al., A composite from poly(m-phenylenevinylene-co-2,5-dioctoxy-p-phenylenevinylene) and carbon nanotubes: a novel material for molecular optoelectronics, Adv. Mater. 10 (1998) 1091–1093, https://doi.org/10.1002/(SICI)1521-4095(199810)10:14<1091::AID-ADMA1091>3.0.CO;2-L.
[15] C. Pramanik, J.R. Gissinger, S. Kumar, H. Heinz, Carbon nanotube dispersion in solvents and polymer solutions: mechanisms, assembly, and preferences, ACS Nano 11 (2017) 12805–12816, https://doi.org/10.1021/acsnano.7b07684.
[16] H. Ago, K. Petritsch, M.S.P. Shaffer, A.H. Windle, R.H. Friend, Composites of carbon nanotubes and conjugated polymers for photovoltaic devices, Adv. Mater. 11 (1999) 1281–1285, https://doi.org/10.1002/(SICI)1521-4095(199910)11:15<1281::AID-ADMA1281>3.0.CO;2-6.
[17] R. Andrews, D. Jacques, D. Qian, T. Rantell, Multiwall carbon nanotubes: synthesis and application, Acc. Chem. Res. 35 (2002) 1008–1017, https://doi.org/10.1021/ar010151m.
[18] C.B. Nielsen, I. McCulloch, Recent advances in transistor performance of polythiophenes, Prog. Polym. Sci. 38 (2013) 2053–2069, https://doi.org/10.1016/j.progpolymsci.2013.05.003.

[19] V. Khomenko, E. Frackowiak, F. Béguin, Determination of the specific capacitance of conducting polymer/nanotubes composite electrodes using different cell configurations, Electrochim. Acta 50 (2005) 2499–2506, https://doi.org/10.1016/j.electacta.2004.10.078.

[20] R. Oraon, A. De Adhikari, S.K. Tiwari, G.C. Nayak, Enhanced specific capacitance of self-assembled three-dimensional carbon nanotube/layered silicate/polyaniline hybrid sandwiched nanocomposite for supercapacitor applications, ACS Sustain. Chem. Eng. 4 (2016) 1392–1403, https://doi.org/10.1021/acssuschemeng.5b01389.

[21] T.P. Kaloni, P.K. Giesbrecht, G. Schreckenbach, M.S. Freund, Polythiophene: from fundamental perspectives to applications, Chem. Mater. 29 (2017) 10248–10283, https://doi.org/10.1021/acs.chemmater.7b03035.

[22] G.D.M.R. Dabera, K.D.G.I. Jayawardena, M.R.R. Prabhath, I. Yahya, Y.Y. Tan, N. A. Nismy, H. Shiozawa, M. Sauer, G. Ruiz-Soria, P. Ayala, V. Stolojan, A.A.D. T. Adikaari, P.D. Jarowski, T. Pichler, S.R.P. Silva, Hybrid carbon nanotube networks as efficient hole extraction layers for organic photovoltaics, ACS Nano 7 (2013) 556–565, https://doi.org/10.1021/nn304705t.

[23] Ö. Karatepe, Y. Yildiz, H. Pamuk, S. Eris, Z. Dasdelen, F. Sen, Enhanced electrocatalytic activity and durability of highly monodisperse Pt@PPy-PANI nanocomposites as a novel catalyst for the electro-oxidation of methanol, RSC Adv. 6 (2016) 50851–50857, https://doi.org/10.1039/c6ra06210e.

[24] S. Eris, Z. Daşdelen, F. Sen, Enhanced electrocatalytic activity and stability of monodisperse Pt nanocomposites for direct methanol fuel cells, J. Colloid Interface Sci. 513 (2018) 767–773, https://doi.org/10.1016/j.jcis.2017.11.085.

[25] B. Sen, S. Kuzu, E. Demir, S. Akocak, F. Sen, Polymer-graphene hybride decorated Pt nanoparticles as highly efficient and reusable catalyst for the dehydrogenation of dimethylamine–borane at room temperature, Int. J. Hydrogen Energy 42 (2017) 23284–23291, https://doi.org/10.1016/j.ijhydene.2017.05.112.

[26] B. Philip, J. Xie, A. Chandrasekhar, J. Abraham, V.K. Varadan, A novel nanocomposite from multiwalled carbon nanotubes functionalized with a conducting polymer, Smart Mater. Struct. 13 (2004) 295–298, https://doi.org/10.1088/0964-1726/13/2/007.

[27] S. Yang, D. Meng, J. Sun, Y. Huang, Y. Huang, J. Geng, Composite films of poly(3-hexylthiophene) grafted single-walled carbon nanotubes for electrochemical detection of metal ions, ACS Appl. Mater. Interfaces 6 (2014) 7686–7694, https://doi.org/10.1021/am500973m.

[28] C. Fu, H. Zhou, R. Liu, Z. Huang, J. Chen, Y. Kuang, Supercapacitor based on electropolymerized polythiophene and multi-walled carbon nanotubes composites, Mater. Chem. Phys. 132 (2012) 596–600, https://doi.org/10.1016/j.matchemphys.2011.11.074.

[29] B.S. Ong, Y. Wu, P. Liu, S. Gardner, High-performance semiconducting polythiophenes for organic thin-film transistors, J. Am. Chem. Soc. 126 (2004) 3378–3379, https://doi.org/10.1021/ja039772w.

[30] A. Mandal, A.K. Nandi, Noncovalent functionalization of multiwalled carbon nanotube by a polythiophene-based compatibilizer: reinforcement and conductivity improvement in poly(vinylidene fluoride) films, J. Phys. Chem. C 116 (2012) 9360–9371, https://doi.org/10.1021/jp302027y.

[31] Y. Harel, S. Azoubel, S. Magdassi, J.-P. Lellouche, A dispersability study on poly (thiophen-3-yl-acetic acid) and PEDOT multi-walled carbon nanotube composites using an analytical centrifuge, J. Colloid Interface Sci. 390 (2013) 62–69, https://doi.org/10.1016/j.jcis.2012.09.006.

[32] D. Tuncel, Non-covalent interactions between carbon nanotubes and conjugated polymers, Nanoscale 3 (2011) 3545, https://doi.org/10.1039/c1nr10338e.

[33] X. Hong, Y. Xie, X. Wang, M. Li, Z. Le, Y. Gao, Y. Huang, Y. Qin, Y. Ling, A novel ternary hybrid electromagnetic wave-absorbing composite based on BaFe 11.92 (LaNd) 0.04 O 19 -titanium dioxide/multiwalled carbon nanotubes/polythiophene, Compos. Sci. Technol. 117 (2015) 215–224, https://doi.org/10.1016/j.compscitech.2015.06.022.

[34] J. Zhao, J. Yu, Y. Xie, Z. Le, X. Hong, S. Ci, J. Chen, X. Qing, W. Xie, Z. Wen, Lanthanum and neodymium doped barium ferrite-TiO2/MCNTs/poly(3-methyl thiophene) composites with nest structures: preparation, characterization and electromagnetic microwave absorption properties, Sci. Rep. 6 (2016), https://doi.org/10.1038/srep20496.

[35] Y. Xie, J. Zhao, Z. Le, M. Li, J. Chen, Y. Gao, Y. Huang, Y. Qin, R. Zhong, D. Zhou, Y. Ling, Preparation and electromagnetic properties of chitosan-decorated ferrite-filled multi-walled carbon nanotubes/polythiophene composites, Compos. Sci. Technol. 99 (2014) 141–146, https://doi.org/10.1016/j.compscitech.2014.05.013.

[36] Y. Xie, X. Hong, C. Yu, M. Li, Y. Huang, Y. Gao, J. Zhao, S. Yan, L. Shi, K. Zhang, Q. Lai, Y. Ling, Preparation and magnetic properties of poly(3-octyl-thiophene)/BaFe 11.92 (LaNd) 0.04 O 19 -titanium dioxide/multiwalled carbon nanotubes nanocomposites, Compos. Sci. Technol. 77 (2013) 8–13, https://doi.org/10.1016/j.compscitech.2012.12.017.

[37] M.R. Karim, J.H. Yeum, M.S. Lee, K.T. Lim, Synthesis of conducting polythiophene composites with multi-walled carbon nanotube by the γ-radiolysis polymerization method, Mater. Chem. Phys. 112 (2008) 779–782, https://doi.org/10.1016/j.matchemphys.2008.06.042.

[38] P. Liu, Modifications of carbon nanotubes with polymers, Eur. Polym. J. 41 (2005) 2693–2703, https://doi.org/10.1016/j.eurpolymj.2005.05.017.

[39] L. Liang, W. Xie, S. Fang, F. He, B. Yin, C. Tlili, et al., High-efficiency dispersion and sorting of single-walled carbon nanotubes via non-covalent interactions, J. Mater. Chem. C. 5 (2017) 11339–11368, https://doi.org/10.1039/C7TC04390B.

[40] T.S. Swathy, M.A. Jose, M.J. Antony, AOT assisted preparation of ordered, conducting and dispersible core-shell nanostructured polythiophene – MWCNT nanocomposites, Polymer 103 (2016) 206–213, https://doi.org/10.1016/j.polymer.2016.09.047.

[41] G. Fusco, G. Göbel, R. Zanoni, E. Kornejew, G. Favero, F. Mazzei, et al., Polymer-supported electron transfer of PQQ-dependent glucose dehydrogenase at carbon nanotubes modified by electropolymerized polythiophene copolymers, Electrochim. Acta 248 (2017) 64–74, https://doi.org/10.1016/j.electacta.2017.07.105.

[42] X. Hu, G. Chen, X. Wang, H. Wang, Tuning thermoelectric performance by nanostructure evolution of a conducting polymer, J. Mater. Chem. A. 3 (2015) 20896–20902, https://doi.org/10.1039/C5TA07381B.

[43] (a) M.M. Oliveira, A.J.G. Zarbin, Carbon nanotubes decorated with both gold nanoparticles and polythiophene, J. Phys. Chem. C 112 (2008) 18783–18786, https://doi.org/10.1021/jp8052482;
(b) J. Wan, Y. Si, C. Li, K. Zhang, Bisphenol a electrochemical sensor based on multi-walled carbon nanotubes/polythiophene/Pt nanocomposites modified electrode, Anal. Methods 8 (2016) 3333–3338, https://doi.org/10.1039/c6ay00850j;
(c) M. Feng, R. Sun, H. Zhan, Y. Chen, Decoration of carbon nanotubes with CdS nanoparticles by polythiophene interlinking for optical limiting enhancement, Carbon N. Y. 48 (2010) 1177–1185, https://doi.org/10.1016/j.carbon.2009.11.041;
(d) C.S. Inagaki, M.M. Oliveira, M.F. Bergamini, L.H. Marcolino-Junior, A.J. G. Zarbin, Facile synthesis and dopamine sensing application of three component nanocomposite thin films based on polythiophene, gold nanoparticles and carbon nanotubes, J. Electroanal. Chem. 840 (2019) 208–217, https://doi.org/10.1016/j.jelechem.2019.03.066;
(e) S. Dhibar, C.K. Das, Silver nanoparticles decorated polyaniline/multiwalled carbon nanotubes nanocomposite for high-performance supercapacitor electrode, Ind. Eng. Chem. Res. 53 (2014) 3495–3508, https://doi.org/10.1021/ie402161e;
(f) I. Ebrahimi, M.P. Gashti, Polypyrrole-MWCNT-Ag composites for electromagnetic shielding: comparison between chemical deposition and UV-reduction approaches, J. Phys. Chem. Solids 118 (2018) 80–87, https://doi.org/10.1016/j.jpcs.2018.03.008.

[44] (a) A. Patole, G. Lubineau, Carbon nanotubes with silver nanoparticle decoration and conductive polymer coating for improving the electrical conductivity of polycarbonate composites, Carbon N. Y. 81 (2015) 720–730, https://doi.org/10.1016/j.carbon.2014.10.014;
(b) A. Patole, I.A. Ventura, G. Lubineau, Thermal conductivity and stability of a three-phase blend of carbon nanotubes, conductive polymer, and silver nanoparticles incorporated into polycarbonate nanocomposites, J. Appl. Polym. Sci. 132 (2015), https://doi.org/10.1002/app.42281.

[45] M. Jinish Antony, C. Albin Jolly, K. Rohini Das, T.S. Swathy, Normal and reverse AOT micelles assisted interfacial polymerization for polyaniline nanostructures, Colloid. Surf. Physicochem. Eng. Asp. 578 (2019), https://doi.org/10.1016/j.colsurfa.2019.123627.

[46] M.A. Jose, S. Varghese, M.J. Antony, *In situ* chemical oxidative polymerisation for ordered conducting polythiophene nanostructures in presence of dioctyl sodium sulfosuccinate, IJC-A 55A (2016) 291–297.

[47] J. Jang, H. Yoon, Formation mechanism of conducting polypyrrole nanotubes in reverse micelle systems, Langmuir 21 (2005) 11484–11489, https://doi.org/10.1021/la051447u.

[48] H. Yoon, M. Chang, J. Jang, Sensing behaviors of polypyrrole nanotubes prepared in reverse microemulsions: effects of transducer size and transduction mechanism, J. Phys. Chem. B 110 (2006) 14074–14077, https://doi.org/10.1021/jp061423b.

[49] M. Kotlarchyk, J.S. Huang, S.H. Chen, Structure of AOT reversed micelles determined by small-angle neutron scattering, J. Phys. Chem. 89 (1985) 4382–4386, https://doi.org/10.1021/j100266a046.

[50] H. Li, B. Zhou, Y. Lin, L. Gu, W. Wang, K.A.S. Fernando, et al., Selective interactions of porphyrins with semiconducting single-walled carbon nanotubes, J. Am. Chem. Soc. 126 (2004) 1014–1015, https://doi.org/10.1021/ja037142o.

[51] D. Baskaran, J.W. Mays, M.S. Bratcher, Noncovalent and nonspecific molecular interactions of polymers with multiwalled carbon nanotubes, Chem. Mater. 17 (2005) 3389–3397, https://doi.org/10.1021/cm047866e.

[52] R. Yang, Z. Tang, J. Yan, H. Kang, Y. Kim, Z. Zhu, et al., Noncovalent assembly of carbon nanotubes and single-stranded DNA: an effective sensing platform for probing biomolecular interactions, Anal. Chem. 80 (2008) 7408–7413, https://doi.org/10.1021/ac801118p.

[53] J. Zhang, H. Zou, Q. Qing, Y. Yang, Q. Li, Z. Liu, X. Guo, Z. Du, Effect of chemical oxidation on the structure of single-walled carbon nanotubes, J. Phys. Chem. B 107 (2003) 3712–3718, https://doi.org/10.1021/jp027500u.

[54] S. Osswald, M. Havel, Y. Gogotsi, Monitoring oxidation of multiwalled carbon nanotubes by Raman spectroscopy, J. Raman Spectrosc. 38 (2007) 728–736, https://doi.org/10.1002/jrs.1686.

[55] F. Avilés, J.V. Cauich-Rodríguez, L. Moo-Tah, A. May-Pat, R. Vargas-Coronado, Evaluation of mild acid oxidation treatments for MWCNT functionalization, Carbon N. Y. 47 (2009) 2970–2975, https://doi.org/10.1016/j.carbon.2009.06.044.

[56] A.G. Osorio, I.C.L. Silveira, V.L. Bueno, C.P. Bergmann, H2SO4/HNO3/HCl-Functionalization and its effect on dispersion of carbon nanotubes in aqueous media, Appl. Surf. Sci. 255 (2008) 2485–2489, https://doi.org/10.1016/j.apsusc.2008.07.144.

[57] L. Stobinski, B. Lesiak, L. Kövér, J. Tóth, S. Biniak, G. Trykowski, et al., Multiwall carbon nanotubes purification and oxidation by nitric acid studied by the FTIR and electron spectroscopy methods, J. Alloy. Comp. 501 (2010) 77–84, https://doi.org/10.1016/j.jallcom.2010.04.032.

[58] K. Jiang, A. Eitan, L.S. Schadler, P.M. Ajayan, R.W. Siegel, N. Grobert, M. Mayne, M. Reyes-Reyes, H. Terrones, M. Terrones, Selective attachment of gold

nanoparticles to nitrogen-doped carbon nanotubes, Nano Lett. 3 (2003) 275–277, https://doi.org/10.1021/nl025914t.
[59] S. Kundu, Y. Wang, W. Xia, M. Muhler, Thermal stability and reducibility of oxygen-containing functional groups on multiwalled carbon nanotube surfaces: a quantitative high-resolution xps and TPD/TPR study, J. Phys. Chem. C 112 (2008) 16869–16878, https://doi.org/10.1021/jp804413a.
[60] R. Liu, Z. Liu, Polythiophene: synthesis in aqueous medium and controllable morphology, Sci. Bull. 54 (2009) 2028–2032, https://doi.org/10.1007/s11434-009-0217-0.
[61] A. Gök, M. Omastová, A.G. Yavuz, Synthesis and characterization of polythiophenes prepared in the presence of surfactants, Synth. Met. 157 (2007) 23–29, https://doi.org/10.1016/j.synthmet.2006.11.012.
[62] X. Qiao, X. Wang, Z. Mo, The FeCl3-doped poly(3-alkyithiophenes) in solid state, Synth. Met. 122 (2001) 449–454, https://doi.org/10.1016/S0379-6779(00)00587-7.
[63] P. Jindal, S. Pande, P. Sharma, V. Mangla, A. Chaudhury, D. Patel, B.P. Singh, R. B. Mathur, M. Goyal, High strain rate behavior of multi-walled carbon nanotubes-polycarbonate composites, Compos. B Eng. 45 (2013) 417–422, https://doi.org/10.1016/j.compositesb.2012.06.018.
[64] G. Ma, X. Liang, L. Li, R. Qiao, D. Jiang, Y. Ding, H. Chen, Cu-doped zinc oxide and its polythiophene composites: preparation and antibacterial properties, Chemosphere 100 (2014) 146–151, https://doi.org/10.1016/j.chemosphere.2013.11.053.
[65] V. Datsyuk, M. Kalyva, K. Papagelis, J. Parthenios, D. Tasis, A. Siokou, I. Kallitsis, C. Galiotis, Chemical oxidation of multiwalled carbon nanotubes, Carbon N. Y. 46 (2008) 833–840, https://doi.org/10.1016/j.carbon.2008.02.012.
[66] R. Saito, M. Hofmann, G. Dresselhaus, A. Jorio, M.S. Dresselhaus, Raman spectroscopy of graphene and carbon nanotubes, Adv. Phys. 60 (2011), https://doi.org/10.1080/00018732.2011.582251, 413–550.
[67] R. Schönfelder, F. Avilés, A. Bachmatiuk, J.V. Cauich-Rodriguez, M. Knupfer, B. Büchner, M.H. Rümmeli, On the merits of Raman spectroscopy and thermogravimetric analysis to asses carbon nanotube structural modifications, Appl. Phys. Mater. Sci. Process 106 (2012) 843–852, https://doi.org/10.1007/s00339-012-6787-8.
[68] M.S. Dresselhaus, A. Jorio, M. Hofmann, G. Dresselhaus, R. Saito, Perspectives on carbon nanotubes and graphene Raman spectroscopy, Nano Lett. 10 (2010) 751–758, https://doi.org/10.1021/nl904286r.
[69] I.D. Rosca, F. Watari, M. Uo, T. Akasaka, Oxidation of multiwalled carbon nanotubes by nitric acid, Carbon N. Y. 43 (2005) 3124–3131, https://doi.org/10.1016/j.carbon.2005.06.019.
[70] D.N. Futaba, T. Yamada, K. Kobashi, M. Yumura, K. Hata, Macroscopic wall number analysis of single-walled, double-walled, and few-walled carbon nanotubes by X-ray diffraction, J. Am. Chem. Soc. 133 (2011) 5716–5719, https://doi.org/10.1021/ja2005994.
[71] A. Cao, C. Xu, J. Liang, D. Wu, B. Wei, X-ray diffraction characterization on the alignment degree of carbon nanotubes, Chem. Phys. Lett. 344 (2001) 13–17, https://doi.org/10.1016/S0009-2614(01)00671-6.
[72] L. Tang, F. Duan, M. Chen, Silver nanoparticle decorated polyaniline/multiwalled super-short carbon nanotube nanocomposites for supercapacitor applications, RSC Adv. 6 (2016) 65012–65019, https://doi.org/10.1039/C6RA12442A.
[73] B. Senthilkumar, P. Thenamirtham, R. Kalai Selvan, Structural and electrochemical properties of polythiophene, Appl. Surf. Sci. 257 (2011) 9063–9067, https://doi.org/10.1016/j.apsusc.2011.05.100.
[74] R. Shvartzman-Cohen, E. Nativ-Roth, E. Baskaran, Y. Levi-Kalisman, I. Szleifer, R. Yerushalmi-Rozen, Selective dispersion of single-walled carbon nanotubes in the presence of polymers: the role of molecular and colloidal length scales, J. Am. Chem. Soc. 126 (2004) 14850–14857, https://doi.org/10.1021/ja046377c.
[75] J.B. Hooper, K.S. Schweizer, Theory of phase separation in polymer nanocomposites, Macromolecules 39 (2006) 5133–5142, https://doi.org/10.1021/ma060577m.
[76] H. Ago, T. Kugler, F. Cacialli, W.R. Salaneck, M.S.P. Shaffer, A.H. Windle, R. H. Friend, Work functions and surface functional groups of multiwall carbon nanotubes, J. Phys. Chem. B 103 (1999) 8116–8121, https://doi.org/10.1021/jp991659y.
[77] A.J. Miller, R.A. Hatton, S.R.P. Silva, Water-soluble multiwall-carbon-nanotube-polythiophene composite for bilayer photovoltaics, Appl. Phys. Lett. 89 (2006) 123115, https://doi.org/10.1063/1.2356115.
[78] J. Wilson, S. Radhakrishnan, C. Sumathi, V. Dharuman, Polypyrrole-polyaniline-Au (PPy-PANi-Au) nano composite films for label-free electrochemical DNA sensing, Sens. Actuators B Chem. 171–172 (2012) 216–222, https://doi.org/10.1016/j.snb.2012.03.019.
[79] E.A. Bazzaoui, G. Lévi, S. Aeiyach, J. Aubard, J.P. Marsault, P.C. Lacaze, SERS spectra of polythiophene in doped and undoped states, J. Phys. Chem. 99 (1995) 6628–6634, https://doi.org/10.1021/j100017a052.
[80] G. Shi, J. Xu, M. Fu, Raman spectroscopic and electrochemical studies on the doping level changes of polythiophene films during their electrochemical growth processes, J. Phys. Chem. B 106 (2002) 288–292, https://doi.org/10.1021/jp013023o.
[81] P. Ranjan, S. Shankar, R. Popovitz-Biro, S.R. Cohen, I. Kaplan-Ashiri, T. Dadosh, et al., Decoration of inorganic nanostructures by metallic nanoparticles to induce fluorescence, enhance solubility, and tune band gap, J. Phys. Chem. C 122 (2018) 6748–6759, https://doi.org/10.1021/acs.jpcc.8b00510.
[82] C.J. Lee, M.R. Karim, M.S. Lee, Synthesis and characterization of silver/thiophene nanocomposites by UV-irradiation method, Mater. Lett. 61 (2007) 2675–2678, https://doi.org/10.1016/j.matlet.2006.10.021.
[83] H. Jiang, K. Moon, Y. Li, C.P. Wong, Surface functionalized silver nanoparticles for ultrahigh conductive polymer composites, Chem. Mater. 18 (2006) 2969–2973, https://doi.org/10.1021/cm0527773.
[84] P. Pascariu, A. Airinei, M. Grigoras, L. Vacareanu, F. Iacomi, Metal–polymer nanocomposites based on Ni nanoparticles and polythiophene obtained by electrochemical method, Appl. Surf. Sci. 352 (2015) 95–102, https://doi.org/10.1016/j.apsusc.2015.03.063.
[85] N. Zhang, X. Yu, J. Hu, F. Xue, E. Ding, Synthesis of silver nanoparticle-coated poly (styrene-co-sulfonic acid) hybrid materials and their application in surface-enhanced Raman scattering (SERS) tags, RSC Adv. 3 (2013) 13740–13747, https://doi.org/10.1039/c3ra40888d.
[86] S. Dhibar, C.K. Das, Electrochemical performances of silver nanoparticles decorated polyaniline/graphene nanocomposite in different electrolytes, J. Alloy. Comp. 653 (2015) 486–497, https://doi.org/10.1016/j.jallcom.2015.08.158.
[87] L. Malassis, R. Dreyfus, R.J. Murphy, L.A. Hough, B. Donnio, C.B. Murray, One-step green synthesis of gold and silver nanoparticles with ascorbic acid and their versatile surface post-functionalization, RSC Adv. 6 (2016) 33092–33100, https://doi.org/10.1039/c6ra00194g.
[88] J. Liao, Y. Zhang, W. Wang, Y. Xie, L. Chang, Preparation of γ-Al 2O 3 sorbents loaded with metal components and removal of thiophene from coking benzene, Adsorption 18 (2012) 181–187, https://doi.org/10.1007/s10450-012-9392-4.
[89] X.G. Li, J. Li, Q.K. Meng, M.R. Huang, Interfacial synthesis and widely controllable conductivity of polythiophene microparticles, J. Phys. Chem. B 113 (2009) 9718–9727, https://doi.org/10.1021/jp901395u.
[90] E.E. Sheina, S.M. Khersonsky, E.G. Jones, R.D. McCullough, Highly conductive, regioregular alkoxy-functionalized polythiophenes: a new class of stable, low band gap materials, Chem. Mater. 17 (2005) 3317–3318, https://doi.org/10.1021/cm050083o.
[91] G. Zotti, S. Zecchin, G. Schiavon, B. Vercelli, A. Berlin, E. Dalcanale, L. Groenendaal, Potential-driven conductivity of polypyrroles, poly-N-alkylpyrroles, and polythiophenes: role of the pyrrole NH moiety in the doping-charge dependence of conductivity, Chem. Mater. 15 (2003) 4642–4650, https://doi.org/10.1021/cm030336i.
[92] B.K. Kuila, K. Park, L. Dai, Soluble P3HT-grafted carbon nanotubes: synthesis and photovoltaic application, Macromolecules 43 (2010) 6699–6705, https://doi.org/10.1021/ma100917p.
[93] M.S. Tamboli, M.V. Kulkarni, R.H. Patil, W.N. Gade, S.C. Navale, B.B. Kale, Nanowires of silver-polyaniline nanocomposite synthesized via in situ polymerization and its novel functionality as an antibacterial agent, Colloids Surfaces B Biointerfaces 92 (2012) 35–41, https://doi.org/10.1016/j.colsurfb.2011.11.006 [b].
[94] Y. Zhan, Y. Ren, X. Wan, J. Zhang, S. Zhang, Dielectric thermally conductive and stable poly(arylene ether nitrile) composites filled with silver nanoparticles decorated hexagonal boron nitride, Ceram. Int. 44 (2018) 2021–2029, https://doi.org/10.1016/j.ceramint.2017.10.147.
[95] M.T. Ramesan, V. Santhi, In situ synthesis, characterization, conductivity studies of polypyrrole/silver doped zinc oxide nanocomposites and their application for ammonia gas sensing, J. Mater. Sci. Mater. Electron. 28 (2017) 18804–18814, https://doi.org/10.1007/s10854-017-7830-5.
[96] J. Hedberg, S. Skoglund, M. Karlsson, I.O. Wallinder, Y.S. Hedberg, Sequential Studies of Silver Released from Silver Nanoparticles in Aqueous Media Simulating Sweat , Laundry Detergent Solutions and Surface Water Aqueous Media Simulating Sweat , Laundry Detergent Solutions and, 2014, https://doi.org/10.1021/es500234y.
[97] I. Liu, R.H. Hurt, Ion release kinetics and particle persistence in aqueous nano-silver colloids, Environ. Sci. Technol. 44 (2010) 2169–2175, https://doi.org/10.1021/es9035557.